THE DESIGN OF A TRAVELING - WAVE TUBE

by

LARRY LEX MOORE

B. S., Kansas State University, 1959

A THESIS

submitted in partial fulfillment of the

requirements for the degree

MASTER OF SCIENCE

Department of Electrical Engineering

KANSAS STATE UNIVERSITY OF
AGRICULTURE AND APPLIED SCIENCE

1960

LD
2668
T4
1960
M66
c.2
Documents

TABLE OF CONTENTS

INTRODUCTION 1

INTRODUCTION TO TRAVELING-WAVE TUBES 2

Description of Traveling-wave Tubes 3

Theory of Traveling-wave Tubes 4

Properties of Slow Waveguiding Circuits 6

Attenuation 9

TRAVELING-WAVE TUBE THEORY AND DESIGN 12

Theory of Interaction Gain 13

Experimental Data used in Design 21

Practical Design Procedure 23

EXPERIMENTAL TUBE DESIGN AND RESULTS 31

Design Considerations 34

Description of the Tube 37

Performance Characteristics 52

ACKNOWLEDGMENT 71

REFERENCES 72

INTRODUCTION

This thesis on "The Design of a Traveling-wave Tube", was written primarily as an introduction to high-frequency amplification devices which employ the interaction gain principle. The writer has attempted in the following sections to provide a logical sequence of steps through the theory, theoretical design and the actual fabrication of a traveling-wave tube amplifier.

In the introduction section, information which is very helpful to the understanding of traveling-wave tube parameters and experimental material used in design is presented. It was hoped that this section would help the unfamiliar reader with the understanding of similar material used directly in later portions of this paper.

Next, this paper deals with traveling-wave tube theory and design. The author has derived the theory of interaction gain in a new, straight-forward way so that the engineer with only a basic knowledge of electromagnetic waves can follow the reasoning. A generalized design procedure is then outlined.

The last part of this paper deals with the actual design of a traveling-wave tube amplifier which is followed through from elementary design to the experimental results of the constructed tube. In this section comparison is made between theoretical and observed results and the resulting conclusions are discussed.

INTRODUCTION TO TRAVELING-WAVE TUBES

Since the discovery of the propagation of electromagnetic waves through space by Hertz and the utilization of this phenomenon for communication purposes by Marconi, the problems of generating such waves and of detecting and amplifying signals have been with us. Solutions for these problems have been found for an enormous range of the frequency spectrum. Vacuum tubes, such as triodes, tetrodes and pentodes, have given excellent performance at frequencies extending from the audio range to a few hundred megacycles per second.

For frequencies above a few hundred megacycles per second, difficulties appear in both tubes and circuits. Special precautions in the design and use of the tubes have to be taken in order to extend their usefulness at these frequencies. At still higher frequencies circuits as well as tubes fail, and it becomes necessary to use new circuit concepts and techniques and to devise new types of vacuum tubes that operate on different physical principles. The new tubes, for example klystrons, make use of electron transit-time effects which are partly responsible for the failure of conventional triodes and multiple element tubes at higher frequencies. Cavity resonators and transmission lines or waveguides replace the low-frequency, lumped-constant resonant circuits and the connecting wires.

For a long time klystrons and magnetrons were the principal types of vacuum tubes which could be used at frequencies from hundreds of megacycles to several tenths of thousands of megacycles, a frequency spectrum usually called the microwave spectrum. In recent years there has appeared a class of microwave tubes that may be described collectively as traveling-wave tubes, a name that originated with

the helix - type traveling-wave tube.

Typical traveling-wave tubes have distinctive features which in certain applications make them far superior to klystrons and magnetrons, their closest relatives. As amplifiers, some have an enormous bandwidth, i.e., no tuning is necessary to amplify signals that spread over a wide frequency band. As oscillators, some have a tremendous electronic tuning range, i.e., variation of oscillating frequency necessitates no circuit tuning but only changes in electrode potentials.

Description of Traveling - wave Tubes

All traveling-wave amplifier tubes are composed essentially of four parts; the electron gun which produces a stream of electrons, the input region where r.f. signal is introduced, the amplifier section where the actual amplification of r.f. signal takes place, and the output region where the amplified signal is taken out of the tube. After the electron stream has passed through these three regions it is collected by means of a collector electrode which is connected to the cathode of the gun through a power supply.

The majority of traveling-wave tubes employ a long solenoid surrounding the tube over most or all of its axial extent. This produces a longitudinal magnetic field which counteracts beam defocusing due to space-charge repulsion and thus prevents loss of electrons to surrounding structures. As with other amplifiers, a traveling-wave tube may be converted into an oscillator by providing a feed-back path between input and the output tube. In many types of traveling-wave tubes such a path exists internally in the amplifier section; in fact, special precautions in tube construction must be taken to avoid this internal feed-back if the tube is to be used as an ampli-

fier. Similarly, as can other vacuum tubes, traveling-wave tube amplifiers and oscillators can be amplitude and frequency modulated and can be used as mixers.

The structure which surrounds the electron stream is different for the various members of the traveling-wave tube family. This structure is called the circuit of the tube, and it may or may not have a profound influence on the electronic phenomena in the tube. In this paper traveling-wave tubes with circuits will be considered. The circuit consists of a waveguiding structure, which has the important property that among its many possible modes of propagation of electromagnetic waves there is at least one whose phase velocity is small compared with the velocity of light. It thus becomes possible to accelerate electrons of the stream to such a velocity that they travel synchronously with the electromagnetic wave through the amplifier section of the tube. If the electromagnetic wave has a component of electric field which is along the path of electron travel, as is the case in most tubes, it is intuitively clear that the longitudinal motion of the electrons will be influenced over relatively long distances of travel through the amplifier section, and that changes in the longitudinal motion will in turn influence the fields. The usefulness of traveling-wave tubes liesin the fact that this interaction can be so arranged that d.c. energy of the electrons is converted into a.c. energy of the electromagnetic waves.

Theory of Traveling-wave Tubes

The traveling-wave tube was called "a constructed complication" by J. R. Pierce, and hence, it is not surprising that several methods of approach have been used to unravel the complicated phenomena in the amplification section of this tube.

The most extensively used method in this country which is due to Pierce, is called the "normal mode method". It consists of simultaneously solving two equations, one relating the r.f. field produced on the circuit by an impressed r.f. current from the electron stream, and the other relative r.f. current produced in the electron stream by an impressed r.f. field from the circuit.

A second method, which was applied by Hahn and Ramo in their investigations of space-charge waves in electron streams, and later by Chu, Jackson and Rydbeck to helix-type traveling-wave tubes, is called the "field method". This method consists of solving Maxwell's equation combined with the Lorentz equation in various regions of the amplification section (i.e., inside the beam, outside the beam but inside the surrounding structure, and outside the surrounding structure) and applying appropriate boundary conditions at the surface separating the various regions.

A third method, which has been used less frequently, may be called the "kinematic method", and is based on energy exchange considerations between the electron beam and the electric fields of the waves.

In the second part of this paper, the author has derived the amplification section theory, using methods and procedures combined from all three methods above. It is the opinion of the writer that this approach presents the simplest, most direct approach presently known.

Properties of Slow Waveguiding Circuits

The literature on this subject is quite extensive. There is, to us, no interest in conventional waveguides filled with a dielectric to reduce the phase velocity of a wave since the electromagnetic field of such structures is concentrated in the dielectric and only a very ineffective field exists in the empty space left for the electron beam to pass through. In all waveguides that are used in traveling-wave tubes a slow phase velocity is obtained by suitable formation of the wall enclosure. These waveguides consist of the helix and other periodically loaded guides of the usual type into which some kind of periodic discontinuities (apertures, disks, bends) are introduced.

The true helix is also a periodic structure. In early traveling-wave tube theory, however, the actual helix was replaced by an idealized cylindrical surface perfectly conducting, but in the helical direction only. This meant that the periodicity given by the pitch of the actual helix was reduced to zero. Recent analysis of the wave propagating properties of an actual helix has explained not only the shortcomings of helix-type traveling tubes, but many of their useful properties.

The properties of periodically loaded waveguides are described mathematically by Maxwell's equation and by the wave equation which may be derived from them. The application of the boundary conditions then leads to an equation for the propagation constants associated with the various complicated geometry of the enclosures. The solutions are usually formidable; however, a few important general properties may be obtained by relatively simple reasoning.

The wave function describing the axial propagating properties of a periodic structure with axial periodicity L must be of the form $e^{-\gamma z}$ multiplied by an arbitrary periodic function of z with period L; an axial displacement of the structure by a distance L can then change the wave function only by a constant factor, here written as $e^{-\gamma l}$. If the arbitrary periodic function is written in the form of a Fourier series, the wave function can be taken as a sum of exponentials, $e^{-(\gamma + 2\pi n j \frac{1}{L})z}$ with appropriate coefficients. In the case of wave guides, γ is either real (attenuated wave) or purely imaginary (progressive unattenuated waves). Writing, in the later case, $\gamma = j\beta_0$, $\beta_0 = \frac{\omega}{v}$ and considering steady state phenomena, the nth Fourier component may be written as $e^{j(\omega t - \beta_n z)}$, where $\beta_n = \beta_0 + \frac{2\pi n}{L}$. Again, because of the periodic nature of the guide, w/c as a function of B_0 must be periodic with period $2\pi/L$ and must be an even function of B_0. Taking these properties into account, $w/c = \frac{\omega}{\sqrt{\mu_0 \epsilon_0}}$ as a function of B_0 must be of the form in Figure 1.

A plot such as Figure 1 is very informative because two important quantities, namely, the phase and group velocity, may be found directly from the graph. The slope of the radius vector from the origin to a point on the curve is equal to the phase velocity Vp divided by the velocity of light c, whereas the slope of the curve at a point is given by $\frac{1}{c}\frac{d\omega}{d\beta_0} = \frac{V_g}{c}$; i.e., it is equal to the group velocity Vg divided by the velocity of light c.

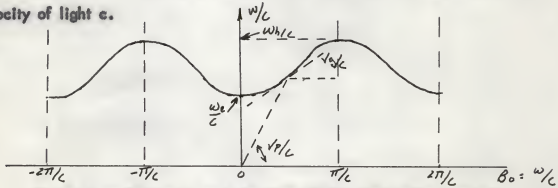

Figure 1 — Frequency as a function of the propagation constant.

Since the Bn are obtained by adding an integral multiple of $2\pi/L$ to B_o, the phase velocity corresponding to the Bn decreases as n increases. Furthermore, by inspecting Figure 1, there are some component waves that exist which have a negative value of group velocity, although the phase velocity has a positive value. Since in structures considered for traveling-wave tubes, the direction of the group velocity is the direction of the energy flow, it is seen that for some component waves the energy flow is in a direction opposite to that of the phase velocity. These waves are called the "backward waves" and have recently been utilized in one of the most important types of traveling-wave tubes, the backward wave oscillator.

From Figure 1 it was also seen that there are two frequencies corresponding to $\frac{\omega_h}{c}$ and $\frac{\omega_s}{c}$ for which the group velocity, Vg, is equal to zero. This means that for these two frequencies there is no propagation of energy. As a matter of fact, there exists a whole band of frequencies above this wh/c for which no propagation exists; beyond this band there is again one for which propagation takes place, and this picture repeats itself. The totality of all the branches belong to one possible mode of the unloaded guide and other modes produce similar bands of propagation and non-propagation. For traveling-wave tubes, only the lowest branch of the lowest mode is utilized, in order to avoid the problem of mode interference.

It may be said that the periodically loaded guide has the properties of a filter. The component waves belonging to the Bn are called space harmonics or Hartree harmonics; they are of importance in many fields of physics.

As was mentioned before, the computation of B_o as a function of w is a task which is nearly impossible to carry out rigorously for most loaded guides. In most

cases assumptions and approximations must be made which can often be justified only by experimental tests of the results.

The waveguiding structure most often used for traveling-wave tubes is the helical waveguide. The theory of this guide was most fully developed by Sensiper and then extended by Watkins. Fletcher has since modified Sensiper's and Watkins' papers to make allowances for the modifications of the waveguides surrounding.

Attenuation

Attenuation must be provided in traveling-wave tubes to prevent oscillations due to waves which are reflected from output mismatches back to the input region. These reflections will of course be amplified and lead to unstable oscillation of the amplifier. In helix-type tubes the attenuation is usually provided by applying aquadag or pyrolytic carbon on the ceramic rods which support the helix or on the outside of the glass tubing which surrounds the helix. The coating of attenuating material is often tapered in thickness and shape to prevent reflections of waves from the attenuator inputs. This is very important since multiple reflections from the input and output matching sections and from the attenuator may cause considerable gain variation over the amplifying frequency band of the tube. This small gain variation is very important in low noise tubes as well as in systems where isolation is needed when the tube is inoperative.

Localized attenuation is also produced by coupling the r.f. energy of the electromagnetic wave out of the tube by means of a short section of another helix and then using an attenuating material. The helix is wound in opposite direction to the helix of the tube and is arranged to be concentric with it. It is well known that the power in coupled transmission lines periodically shifts from one line to the other,

the distance between points of complete power transfer being a characteristic of the lines and the coupling between them. If the proper length of oppositely wound helix is placed outside the glass vacuum envelope of the tube, power can be transferred to this external helix and absorbed by some convenient method. More information on attenuation may be found in Pierce's "Traveling-wave Tubes". Figure 2 shows a diagram of the relative power levels at each point of a typical traveling-wave tube.

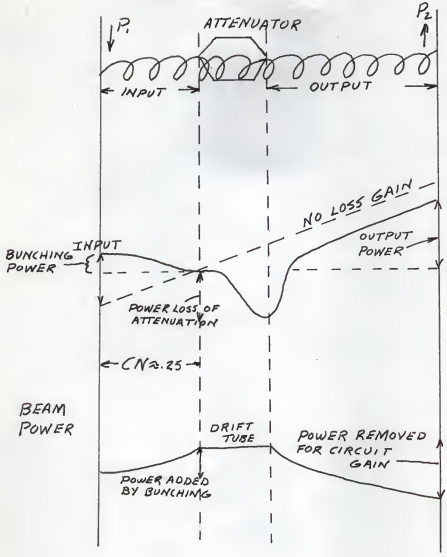

Figure 2 — Relative power levels at each point on a typical traveling-wave tube.

TRAVELING-WAVE TUBE THEORY AND DESIGN

It has been attempted in this section, to present a simple, straight-forward derivation of traveling-wave interaction theory and to introduce the various information on traveling-wave tube parameters used in the design of the actual tube. The basic theory of interaction gain is derived by making a number of justified assumptions which allow the engineer, with only a basic knowledge of electromagnetic wave theory, to interpret the feasibility of employing this method of amplification for microwave devices. The wave equations of the beam and slow wave structure are solved assuming both simple propagation constants and propagation constants which involve experimental parameters. This method of approach is followed to completion by arriving at an equation which will determine the magnitude of gain on any slow-wave interaction device.

Traveling-wave tube design is largely a compromise between experimental results and derived theory. Many of the traveling tube parameters are determined both experimentally and theoretically and are then chosen, where there is conflict, by reference to past experience. This design procedure, which may sound very unrigorous, gives quite good results when used by an engineer with adequate experience in microwave devices.

It has not been attempted, in this section, to justify or defend the idealness of the curves and parameters presented as references for design. This was purposely done since in the last part of this report the author has made these comparisons by using the experimental results of an actual tube designed employing the design procedure presented on these pages. This type of comparison, of course, is the final criterion for the evaluation of any design procedure.

Theory of Interaction Gain

Wave analysis of circuit and electron stream. In order to derive expressions for the electronic and circuit equations the following assumptions and terms must be presented.

I_0 = Beam Current
V_0 = Beam Voltage
N = Number of active wavelengths on circuit
L = Axial length of the circuit
λ_0 = Free space wavelength
V_p = Phase velocity of wave along the circuit
C = Velocity of light

Assume:

1. Constant velocity, volume and charge density across the beam
2. A very thin electron stream
3. All flow of electron is in the axial direction
4. It is assumed that all a-c quantities vary as $e^{-jbz}\, e^{jwt}$

Terms defined:

Charge Density	$-P_{dc} + P_{ac} = -P_o + P = P^1$
Convection Current	$-i_{dc} + i_{ac} = -I_o + i = i^1$
Velocity	$+U_{dc} + U_{ac} = -U_o + U = V^1$
Current Defined	$i^1 = P^1 V^1$ = charge density x velocity
	$i^1 = (-I_o + i) = (-P_o + P)(-U_o + U) =$
	$\frac{\text{Coul/sec}}{M^2}$
Expanded	$i^1 = \underbrace{+P_o U_o}_{dc = I_o} + \underbrace{(PU_o - P_o U)}_{ac = i} + \underbrace{PU}_{''}$

for small signal analysis we can neglect a.c. products compared with (ac) (dc) products.

$$I = I^1 = P_o U_o + P U_o - P_o U$$
$$I^1 = P_o (U_o - U) + P U_o \qquad -V = U_o - U$$
$$I^1 = -P_o V + P U_o$$

$$P = \frac{I^1 + P_o V}{U_o} \qquad \text{(Equation one)}$$

However, variation was assumed only in the Z or axial direction

$$\frac{\partial i}{\partial z} = -\frac{\partial \rho}{\partial t}$$

Let B_I = some constant

$$-j\beta_i = -j\omega\rho \qquad \beta_i = \omega\rho \qquad \text{(Equation two)}$$

Combining I and II $\quad i = \dfrac{-\omega\rho_o v}{\omega - \beta u_o}$ $\qquad$ (Equation three)

This is convection current density

From Newton's second law for the case of only Z displacement

$$m\, dv/dt = F = -eE = \left[\frac{\partial v}{\partial t} + (u_o + u)\, dv/dz \right] m$$

$$v = \frac{-e}{m} E \Big/ j(\omega - \beta u_o) \qquad \text{(Equation four)}$$

Now from Newton's second and Convection current density

$$i = -j \frac{e/m\, \omega \rho_o E}{(\omega - \beta u_o)^2} \qquad \text{(Equation five)}$$

Total current density (ac) $\qquad i_t = i + i_d \qquad i_d = \epsilon \dfrac{dE}{dt}$

$i_t = i + \epsilon \dfrac{dE}{dt} = i + j\omega\epsilon E$ $\qquad$ Now add this term to I(Equation five)

$$i_{total} = \frac{-j\, e/m\, \omega \rho_o E}{(\omega - \beta u_o)^2} + j\omega\epsilon E \qquad \text{(Equation six)}$$

Defined term $\quad e/m\, \rho_o \triangleq \epsilon \omega_p^2$

$$\omega_p^2 \triangleq \frac{e}{m} \rho_o / \epsilon \qquad \text{Radian Plasma Frequency}$$

Displacement current is again $i + i = i_t \qquad i_t = \nabla \times H = i + \partial D/\partial t$

$$\nabla \cdot \nabla \times H = \nabla \cdot i_t$$

From high frequency considerations by Ramo i_1 is zero

$$\therefore\ i_1 = 0$$

Now if we substitute the value of Wp in equation six

$$-\frac{j\epsilon\omega_p^2\omega E}{(\omega-\beta u_0)^2} = -j\omega\epsilon E$$

now $(\omega-\beta u_0)^2 = \omega_p$

Now if solved by Quadratic Equation

$$\beta = \frac{\omega}{u_0} \pm \omega_p/u_0 \qquad \text{(Equation seven)}$$

In actual circuits Wp = Wg/R, where R is plasma reduction factor

B can now be defined as $\beta = \omega/v$ so $v = \omega/\beta$

From equation seven

$$v = \frac{\omega}{\frac{\omega}{u_0} \pm \frac{\omega_p}{u_0}} = \frac{\omega u_0}{\omega \pm \omega_p} = \frac{u_0}{1+\omega_p/\omega} \qquad \text{(Equation eight)}$$

This defines two waves:

1. One slow wave for the + case = V_1
2. One fast wave for the − case = V_2

These are space change waves

$$V_1 = U_0/1 + Wp/w$$
$$V_2 = U_0/1 - Wp/w$$

The slow wave is used for interaction.

<u>Electronic Equation</u>. It is assumed:

1. no transverse motion
2. small signals
3. r.f. current is uniform across the cross-section
4. signals vary by $e^{j\omega t}$

Three equations will also be used;

a. Continuity $\partial i/\partial z = -j\omega\rho$

b. Definition of current $i = \rho_0(u+u_0) + \rho u_0$

c. Equation of motion $-\frac{e}{m}E = j\omega v + u_0\,\partial v/\partial z$

(A) $\frac{\partial v}{\partial z} = -j\omega\rho$ Now if this equation is combined with equation (B)

$$I = \rho_0 v + \rho u_0 = \rho_0 v - (u_0/j\omega)(\partial i/\partial z)$$

Now if this equation is substituted into the equation of motion

$$-\frac{e}{m}E = j\omega\left[\frac{i}{\rho_0} + \frac{u_0}{j\omega\rho_0}\frac{\partial i}{\partial z}\right] + u_0\left[\frac{i}{\rho_0}\frac{\partial i}{\partial z} + \frac{u_0}{j\omega\rho_0}\frac{\partial i^2}{\partial z^2}\right] \quad \text{(Equation nine)}$$

This is the basis for the Electronic Equation

Now define $B_0 = \frac{W}{U_0}$ and

$$KE = PE \qquad \frac{1}{2}m u_0^2 = eV_0 \qquad \frac{m u_0^2}{e} = -2V_0$$

and I_0 (total current) = (cross section)(charge density)(velocity)

$$I_0 = \rho_0 U_0$$

$$\rho_0 = I_0 / G U_0$$

Using these different definitions:

$$\partial^2 i/\partial z^2 + 2j\beta_e \frac{\partial i}{\partial z} - \beta_e^2 i = j\frac{\beta_e I_0}{2eV_0}E \quad \text{(Equation ten)}$$

This is the relation between the electric field and the beam electrons and is referred to as the electronic equation. It gives the relation of the effect of the circuit on the beam - the circuit fields act on the beam only by this function.

<u>Circuit Equation.</u> This equation gives the effect of the beam on the circuit.

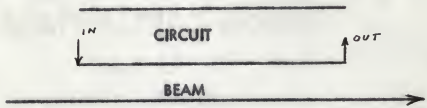

Figure 3 — A diagram of the beam and circuit

Consider a sliced beam — This is the situation of having a current generator

which induces a field (currents) on the circuit. It will set up waves going in both directions. The relation which represents the interaction between the beam and circuit fields is called the interaction impedance. This will again be considered in the tube design procedure.

The propagation constants are: β_o = W/V circuit
β_e = W/U_o beam

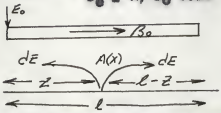

Figure 4 — A diagram to show currents induced on the circuit.

E (total electric field) = $E_o e^{-j\beta_o z} + \int_0^z \frac{1}{2} A(x) e^{-j\beta_o(z-x)} dx + \int_z^\ell \frac{1}{2} A(x) e^{-j\beta_o(x-z)} dx$

Differentiate this by special formula. Use the Leibnitz rule with respect to Z.

This is of the form: $\frac{d}{dz}\int_a^b f(x,z)\,dx = \int_a^b \frac{\partial f(x,z)}{\partial z} dx + f(b,z)\frac{db}{dz} - f(a,z)\,da/dz$

$$\frac{dE^2}{dz^2} + \beta_o^2 E = j\beta_o A(z)$$ (Equation eleven)

By inspection of the circuit dE = $\frac{1}{2} A(z)\,dz$

Definition of power on circuit is $P_c = E^2 / 2\beta_o^2 K$

Where E^2 is the peak electric field on axis
K is the interaction impedance
β_o is the circuit propagation constant

The rate of power increase on circuit is:

$$dP_c = dP_b \qquad dP_c = \frac{2E\,dE}{2\beta_o^2 K} = \frac{E\,dE}{\beta_o^2 K}$$

dP_b = rate of decrease of power in beam $\quad dE = \frac{1}{2} A(z)\,dz$

$dP_b/dz = \frac{1}{2} F(x,\gamma) E\,dz$ $\qquad \gamma$ = cross sectional area

$$\frac{E\,dE}{\beta_o^2 K} = -\frac{1}{2} F(x,\gamma) E\,dz \qquad dE = -\frac{\beta_o^2 K}{2} F(x,\gamma)\,dz$$

Again from inspection of the circuit dE = 1/2 A (Z) dZ

$$\tfrac{1}{2} A(z)\,dz = -\beta_0^2 K F(\mu,\gamma)\,dz \qquad A(z) = -\beta_0^2 K F(\mu,\gamma)$$

Now substitute into equation eleven.

$$d^2E/dz^2 + j\beta_0^2 E = j\beta_0^3 K F(\mu,\gamma)$$

This is the circuit equation.

<u>Solving of the Electronic and Circuit Equations for Wave Propagated.</u> In the previous work unvarying beams and circuit voltages were assumed. Now, in order to solve for the propagation constants it is assumed:

1. $I = Ae^{-\Gamma z}$
2. $E = Be^{-\Gamma z}$

The electronic equation with these assumptions becomes:

$$\Gamma^2 i - 2j\beta_e \Gamma i - \beta_e^2 i = j\frac{\beta_e I_0 E}{2GV_0} \qquad \frac{I}{E} = -j\frac{\beta_e I_0 / 2GV_0}{(j\Gamma + \beta_e)^2}$$

The circuit equation with the same assumptions becomes:

$$i/E = \frac{\Gamma^2 + \beta_0^2}{j\beta_0^3 K G}$$

If these two equations are now set equal it will be possible to solve for the propagation constants.

$$\frac{\Gamma^2 + \beta_0^2}{\beta_0^3} = \frac{\beta_e I_0}{2V_0(\beta_e + j\Gamma)^2}$$

This equation is in the admittance form since the two equations equated are the ratios of I / E.

If the above expression is graphed it will give an excellent insight into the roots of this equation

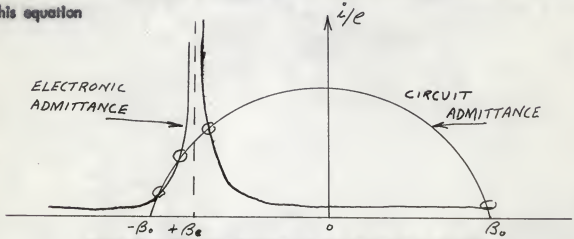

Figure 5 — Graphic Solution of the Interaction Equation.

As may be seen the roots of this equation are represented by the points of curve intersection. As may be seen from the diagram the number of roots depend on the magnitude of the interaction impedance, K, since this term will raise or lower the circuit admittance curve. The same effect would result if I_o (beam current) is variable.

The equation expressing the roots may be written

$$(\beta_e + j\Gamma)^2(\beta_e^2 + \Gamma^2) - \beta_o^3 \beta_e K I_o / 2V_o = 0$$

This equation will now be solved for its roots at synchronous voltage. $B_e = B_o$. This expression shows equal velocities for V_p of the circuit and beam. For simplification the following expression defined by Pierce will be used. $C^3 = \frac{I_o K}{4V_o}$

<u>Assuming Simple Propagation Constants.</u> Assume the solution

$$j\Gamma = -\beta_e(1 + jC\delta) \quad jC\delta << 1 \qquad (-j\beta_e C\delta)^3(2\beta_e + j\beta_e C\delta) - 2\beta_e^4 C^3 = 0$$

$$2j\beta_e^4 C^3 \delta^3 = 2\beta_e^4 C^3 \qquad j\delta^3 = 0 \quad \text{OR} \quad \delta^3 = -j^0$$

The backward wave root was neglected to reduce the equation. This was done with the knowledge that this wave was of very little interest to us. The remaining three roots are:

$$s_1 = e^{-j\pi/6} = \sqrt{3}/2 - j\,1/2$$
$$s_2 = e^{-j5\pi/6} = -\sqrt{3}/2 - j\,1/2$$
$$s_3 = e^{j\pi/2} = j^0$$

These will now give the following answers to the assumed solutions.

1. $\Gamma_1 = j\beta_e - C\beta_e(\sqrt{3}/2 - j\,1/2)$
2. $\Gamma_2 = j\beta_e - C\beta_e(-\sqrt{3}/2 - j\,1/2)$
3. $\Gamma_3 = j\beta_e - C\beta_e(j)$

It was assumed that the waves vary by $e^{-\Gamma z}$. If the real part of $R_e(\Gamma) > 0$ there is attenuation, if the real part of $R_e(\Gamma) < 0$ there is a growing wave.

1. Γ_1 REAL PART IS − SO GIVES GAIN
2. Γ_2 REAL PART IS + SO DECAYS
3. Γ_3 REAL PART IS ZERO

Γ_1 is the growing wave that the engineer is interested in employing in gain devices.

<u>Propagation Constants using Experimental Parameters.</u> In the previous work the author has derived a simple solution to the interaction between the traveling-wave tube beam and its slow-wave structure. In this, a cubic equation was obtained by rejecting the backward wave and the equation reduced to the form S = −j. Only one mode was assumed in this solution. In actual design many modes are present, as well as circuit loss, which should be taken into account.

The passive mode parameter Q was introduced by Pierce for accounting for many modes and circuit loss. Pierce re-analyzed the problem and wrote the propagation constant as $j\Gamma = \beta_e[1 + cb - jd]$ where

- b is the velocity parameter which allows for the difference between the circuit and beam velocity
- d is the loss parameter which accounts for circuit loss
- c is the Pierce gain parameter $C^3 = I_0 K / 4V_0$

When one goes through the derivation using the correction factors the following is obtained:

$$\underset{(a)}{\left(\delta + j\frac{\sqrt{Qc}}{1-\sqrt{4Qc}}\right)}\underset{(b)}{\left(\delta - j\frac{\sqrt{4Qc}}{1+\sqrt{4Qc}}\right)}\underset{(c)}{\left(\delta + jb + d\right)}$$

$$\underset{(a)}{\left(\delta - jb - d - 2j/c\right)} = \underset{(c)}{(\delta - j/c)^2 2c}\left(1 + \frac{cb + jcd}{1 - 4Qc^3}\right)$$

The roots of this are:

a. the slow space charge wave
b. the fast space charge wave
c. the forward circuit wave
d. the backward circuit wave

This is the most accurate equation now used and is applicable to any slow-wave structure.

Derivation of the gain equation used for the design of traveling-wave tubes.

Assume the following boundary conditions.

At $Z = 0$ $\quad V = 0$, $I = 0$ $\quad E = E_0$

Γ_2 AND Γ_3 can be neglected since Γ_1 is much larger in magnitude.

The gain of the growing wave is given by: $G = 20 \log_{10} e^{(\beta_c C \sqrt{3}/2)\ell}$

Define $N = \ell/\lambda_c$ $\quad \lambda_c = \frac{2\pi}{\beta_c} = \frac{V_0}{f}$ stream wave length

The gain is now: $G = 20 \log_{10} e^{2\pi C N \sqrt{3}/2} = 47.3\, C N$

Approximately 1/3 of the field applied (input) is all which will have gain.

Power in $\approx \left(\frac{E_1}{3} + \frac{E_2}{3} + \frac{E_3}{3}\right)^2$ $\quad \frac{1}{9}$ of power in is in the growing wave. $A = 10 \log_{10} 1/9 = -9.54$ db

Gain is $A + B\,C\,N$
Gain is $-9.54 + 47.3\,C\,N$

Experimental Data used in Design

The design procedure outlined in this section is representive of the typical considerations which are made during the basic design of traveling-wave tube amplifiers and backward-wave oscillators. This procedure is based primarily on small signal gain considerations but is does, however, give accurate approximations to actual operation parameters. It is also necessary, in the procedure, to determine the values of certain r.f. propagation characteristics of the slow - wave structure used in the tube. With experience and adequate facilities these characteristics may be determined from cold slow - wave structure measurements, thus eliminating the expense of measurements on complete TWT's with electron beams. This would, of course, be the final criterion for any measurement system.

Measurements, which may be made on the slow-wave structure, will yield the following parameters:

1. Phase velocity and phase velocity dispersion
2. Attenuation
3. Phase velocity under attenuator
4. Stop-band details
5. Interaction impedance
6. Cold synchronous voltage

Other quantities may be derived from these measurements using appropriate theoretical considerations, such as:

7. Dielectric loading factor
8. Matching impedance

Phase velocity is obtained easily and accurately at any frequency using a technique based on the fact that a coupling helix may be made to act as a selective, high reactance for a helical structure. By proper adjustment of the coupling helix, the wave length of the first forward wave or the first backward wave harmonic may be measured by standing wave-probing methods. By a similar technique, the perturbation of wavelength caused by a dielectric rod inserted into the helix can be measured and interrupted as a measurement of interaction impedance. This technique works on the theory that when a dielectric is placed in a high field region, energy is stored within the dielectric and will thus change the propagation constant. This change in the propagation constant has been expressed in terms of interaction impedance by Lagerstrom. This same parameter can also be found from the dielectric loading factor which can be determined experimentally from phase velocity change. This relation has a two fold value since not only the transverse interaction impedance may be found but the longitudinal impedance is also predictable. It is usually about one-half of the transverse component.

All of the above experimentally measured parameters give the design engineer additional checks on his theoretical calculations. This data also gives "feel" to the engineer, as how to interpret unusual phenomenon encountered during the tube development.

Practical Design Procedure

The traveling-wave tube is usually to be designed as a special purpose tube and this purpose will normally make the specifications for its performance quite critical. Some of the more common limitations are power supply, weight, and size but for simplification the design procedure presented here will assume that only the basic requirements listed below are to be specified.

Frequency Range	2 to 4 KMC
Gain	30 d b minimum
Power Output	X watts minimum
Voltage, operating	Y volts maximum

Each component of the traveling-wave tube will be discussed and after some consideration a value for the parameter of that component will be made. These values will be re-evaluated after the other parameter values in the system are made. As with all complicated devices the final value of the parameters will be a compromise of the original values.

Electron Guns. The guns that are used in traveling-wave tubes are most often convergent guns of the Pierce type with a perveance in the neighborhood of $1X10^{-6}$. Perveance is defined as the ratio of beam current to the 3/2 power of the beam voltage (V_o). The current density limitations that the designer is forced to work between are the ratios of cathode to beam area as a lower limit and the lowest per-

veance possible for an upper limit. The lowest perveance possible means the highest possible V_o that your specifications will allow. In most cases the engineer will use, if possible a gun which has been developed and operate it as close to V_o maximum as possible.

(1) Gun considerations will fix the operating voltage (V_o) used which will be a gun which can operate very close to V_o maximum of your specifications.

(2) The input power requirement will now also fix the input current I_o.

Slow-wave Structures. The operating voltage (V_o) also will determine the approximate turns-per-inch of the helical structure to be used since gain is obtained when the phase velocity of the slow-wave structure and be beam velocity of the gun are approximately equal. The speed of the beam is $= \sqrt{\frac{V_o}{506}}\, C$. Helical structures display very little dispersion and will therefore match one beam voltage for wide frequency range. The following curves in Figure 6 are typical of the experimentally measured helical waveguide dispersion curves. The following parameters are defined: $ka = 2\pi a/\lambda_o$ $k = 2\pi/\lambda_o = \omega/C$ $\lambda_o = \frac{30}{freq}$ $\gamma = \sqrt{\beta^2 - K^2}$
$\gamma \approx \beta$ $\gamma \approx 2\pi/\lambda_s$ $\cot\psi = (2\pi a)(TPi)$

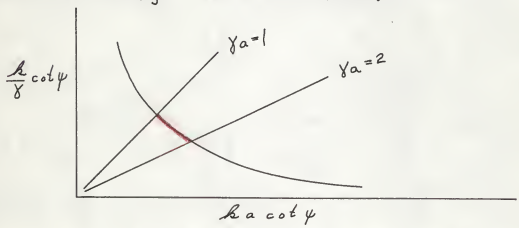

A plot of $k/\gamma \cot\psi$ VS $ka \cot\psi$ AND γa

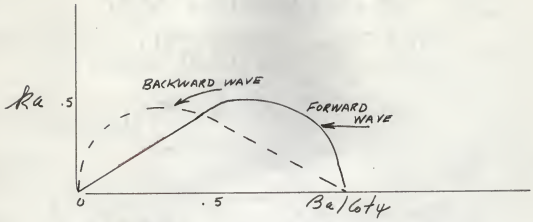

A plot of ka vs $Ba/6t\psi$

Figure 6 — Helical waveguide dispersion curves.

The regions marked in red on the curves in Figure 6 are the desired regions of design from interaction considerations. ka should always be less than .5 since this is the cross-over point for the backward and forward waves. Some thought must now be given to interaction impedance in order for the designer to choose γa, helix radius and turns-per-inch of the helix. From Figures 6 and 7a it is seen that the designer is confronted with a number of conflicts.

1) Low γa is needed for a high interaction impedance (K).

2) Low ka to avoid unwanted interaction.

3) Large K for large helix structures since they have higher power capabilities and ease of construction.

4) Large γa to have constant phase velocity.

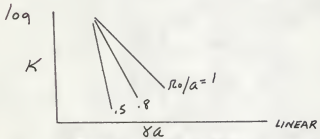

Figure 7a — Plot of K vs γa and r_0/a.

The curves in Figure 6 show the characteristics of the slow—forward wave. The changing radius and turns-per-inch of the helix will only shift the operating position on this curve. In order to raise or lower this curve the environment around the helix must be changed. The measurement of this change, from the free—space position, defines its dielectric loading factor(D L F). From the defining term it is known that $ka \cot\psi$ is a function of frequency and that $\frac{k}{\gamma} \cot\psi$ is a function of phase velocity for a constant helix radius and turns-per-inch. $\frac{ka}{\gamma a} = \frac{V_p}{c}$ The axis $\frac{k}{\gamma} \cot\psi$ can also be scaled as a function of the beam velocity since V_o defines a velocity at which the beam and slow - wave should travel.

$$\frac{V_p}{c} = \frac{\sqrt{V_o}}{506} \quad \text{or} \quad \frac{ka}{\gamma a} = \frac{\sqrt{V_o}}{506}$$

This expression will now give $\frac{ka}{\gamma a}$ from the voltage V_o.

From the backward - wave and fast wave considerations a low ka is desired, since interaction between the beam and any mode except the slow forward—wave is very undesirable.

The following table shows typical values of these parameters in present tubes. All the parameters are shown as mid - band values.

Table 1 Typical and values in T W T's.

Power	ka	γa	V_o
Low-level	.08	2.3	400 Volts
Medium Power	.10	2.2	850 Volts
High Power	.15 - .20	1.1 - 1.5	7,000 to 9,000 volts

From the data that has been considered, and experience, the design engineer can now make a decision on the value of γa. Once this is done ka, r and tpi are easily found from the defining terms.

Determination of Electron Beam Diameter. The E_z field that is used in the interaction processes is the strongest next to the helix. Here again the engineer is faced with a compromise situation on his ideal beam diameter.

1) The beam should be as large as possible for good interaction.

2) The beam should be as small as possible for low helix interception, i.e., low noise.

3) The larger the beam the less focusing power is needed.

4) Holding the beam small will keep down backward wave oscillation since the backward wave power is the strongest near the helix.

A very common value for r_o/a is .5. For higher power tubes r_o/a sometimes runs as low as .3.

The beam diametric is now chosen by considering these parameters and previous experience.

Interaction Impedance. Interaction impedance is defined by Pierce as $K = \frac{E_z^2}{2\beta^2 P}$. As has been seen K is a function of γa and ka and decreases with dielectric loading. The term K_s is used to relate K free space and K in a dielectric. Figure 7b shows $K_s \frac{k}{\gamma}$ vs γa as a function of beam loading.

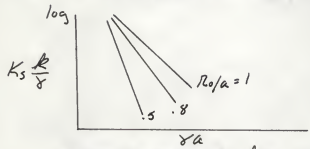

Figure 7 b — Plot of $K_s \frac{k}{\gamma}$ vs γa and r_o/a

These curves were worked out by Tien of Stanford and were computed for a tape helix in a constant dielectric environment. He defines K in his curves as $K = K_s F$

where $F = F_1 F_2$. F is an impedance reduction factor which is actually a ratio of tape impedance with dielectric loading to sheath impedance in free space. F_1 depends on ka and $\frac{S_w}{\text{pitch}} = \frac{\text{tape width}}{\text{pitch}}$ or wire diameter. F_2 depends on the dielectric loading factor. Figure 8 shows Tien's plot of F_1.

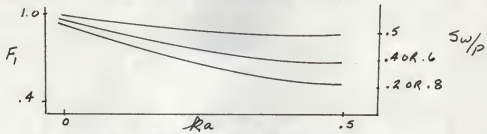

Figure 8 — Plot of F_1 vs ka and S_w/P

From Figure 8 it can be seen that at $ka = .5$ the interaction impedance is as low as possible. This is another reason for a low value of ka.

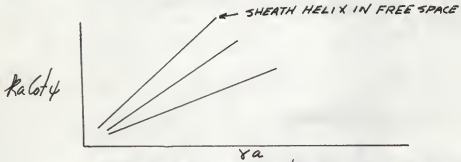

Figure 9 — Plot of $ka \cot\psi$ vs γa with DLF curves

DLF is the ratio of $ka \cot\psi$ of free space to $ka \cot\psi$ of dielectric at a constant γa. From Figure 10 70% of DLF is at an F_2 of .4 and almost one half of the value of K is lost.

Figure 10 — Plot of F_2 vs DLF

A recap of the determination of interaction impedance is:

1) Obtain $K_s \frac{k}{\gamma}$ from Tien's γa vs $K_s \frac{k}{\gamma}$ curve

2) Find F_1 and F_2 from Tien's curves $F = F_1 F_2$

3) Now the actual K is $K_s F$

<u>Gain, Passive Mode and Loss Parameters.</u> In the previous section the author derived a simple solution to the interaction between the T W T beam and slow wave propagating structure. In this, a cubic equation was obtained by rejecting the backward wave and the form $S^3 = jB$ was the resulting equation. In this result only one mode was assumed while in actual design one gets not only many different modes but circuit loss to take into account.

The passive mode parameter Q was introduced by Pierce for solution to these problems. Pierce re-analyzed the problem assuming small loss and wrote the propagation constants as $-j\Gamma = \beta_e [1 + (cb + jcd)]$

b is the velocity parameter which allows for the difference between the circuit and beam velocity.

d is the loss parameter.

c is the Pierce gain parameter. $C^3 = I_0 K / 4 V_0$

k is the interaction impedance

a is the loss factor in setting up a growing wave.

The derivation of this equation using these correction factors yields the following equation

$$\left(S + j\frac{\sqrt{Q}c}{1-\sqrt{4Q}c}\right)\left(S - j\frac{\sqrt{4Q}c}{1+\sqrt{4Q}c}\right)(S + jb + d)(S - jb - d - 2j/c)$$

$$= (S - j/c)^2 2c \left(1 + \frac{cb + jcd}{1 + 4Qc^3}\right)$$

The roots of this are:

(a) Slow space charge wave
(b) Fast space charge wave
(c) Forward circuit wave
(d) Backward circuit wave

Fletcher has devised a method for finding the parameter Q as well as the other parameters of the propagation constant.

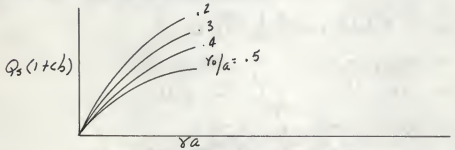

Figure 11 — Plot of Q_s $(1 + cb)$ vs γa

$Q_s = \dfrac{\omega C}{2\beta_e K}$ Q K is a constant for a given structure.

$Q_s K_s = Q K$ $\dfrac{Q_s}{F} = Q$

$Q_s K_s = Q\,(K_s F)$

Velocity parameter b $1 + cb = u_0/v_p$ $\frac{1}{2} m u_0^2 = -eV$

$\therefore\ u_0/c = \sqrt{V/506}$

The cold synchronous voltage is the voltage required to accelerate electrons to velocity V which is the velocity of the circuit wave. Hot synchronous voltage is that voltage which gives optimum gain.

Synchronous Voltage = $V_s = (506\ V/c)^2 = \left(506\ \dfrac{\lambda a}{\gamma a}\right)^2$

Now 1 + C B may be obtained.

Gain

$C^3 = \dfrac{I_0 K}{4V_0}$

I_0 is beam current

V_0 is applied voltage

Birdsall and Brewer have done some very complete work involving Q, C, d and b parameters. They have based the use of their data on finding X_1, which is the real part of the growing wave propagation constant. They have also made some very accurate computations of input losses due to electron bunching and power loss from coupling and beam modulation. From the parameters considered the engineer can obtain these factors X_1 and A from the curves.

$$\text{Gain} = A + B\,C\,N\ \text{db}$$

$$B = \frac{54.6\,X_1}{1 + cb} \qquad N = \ell/\lambda_g$$

If the gain of the tube was specified then $N = \frac{G_s - A}{BC}$ and the length of the tube must be; $\ell = \frac{G_s - A}{BC}\lambda_g$

The preceding design procedure was presented in a very much outlined form. The author was attempting to convey only the basic considerations for each parameter and to list where the interested student can go to find additional information on the determination of each parameter. In the following section, in which the actual design of a traveling-wave tube amplifier was accomplished, the student should gain a better insight as to actual design.

EXPERIMENTAL TUBE DESIGN AND RESULTS

The use of traveling-wave tubes in operating systems has been somewhat limited over the past ten years, however, it now appears that sufficient progress in both tube and system design has been made so that traveling-wave tubes may see widespread application in the near future.

This section describes an experimental helix type traveling-wave tube representative

of a class which could well see extensive use as a power amplifier in radio relay systems. The performance characteristics under nominal operating conditions, for this tube are:

Frequency Range	6000 to 7000 M C
Power Output	5 watts
Gain	34 d b
Noise Figure	< 30 d b

This tube was designed for use with waveguide input and output circuits. The input and output voltage standing wave ratio (V S W R) is less than 1.5 over the band when delivering rated power.

It was endeavored, in developing this tube, to produce a "practical" amplifier for use in relay systems. Such an application requires a high degree of reliability and refinement in performance and demands that the tube be rather conservatively designed. The contemplated system application made it necessary to investigate in detail the problem associated with band flatness, noise, matching, signal distortion and long life.

The solution of some of these problems required the development of a precisely constructed helix assembly and the initiation of a life test program. The results of the life test indicate that life exceeding 9,000 hours can be obtained. This long life is the result of a d.c. profile which minimizes the ion bombardment of the cathode. Permanent magnet focusing circuits were designed for this tube since power consumed by focusing solenoids seriously degrades the overall efficiency of a traveling-wave tube amplifier. To further improve efficiency a collector which can be operated at about half the helix voltage was used.

The difficulties encountered in the course of development were: excessive noise,

ripples in gain-frequency characteristics, and lack of reproducibility of gain. There was evidence that a growing noise current wave on the electron stream was the source of high noise output. This phenomenon has been observed by a number of experimenters but is not yet fully explained. The growing noise wave was eliminated by allowing a small amount of the magnetic focusing flux to link the cathode. Reflections caused by slight non-uniformities in the helix pitch were the source of the gain ripples. The lack of reproducibility in gain was caused by variation in helix attenuation. Careful construction techniques alleviated these problems.

This discussion of the tube was divided into four main parts. The next section discusses some of the many factors affecting the design of the traveling-wave tube. (The abbreviation T W T will be used henceforth.) Values for these parameters were then chosen from the information known about the tube components. The second part describes the actual tube itself and contains certain performance data which is closely related to specific components of the tube. In the third part comparisons are made between the performance predicted from traveling-wave tube theory and that which was actually observed. This type of comparison gives a clear evaluation of the value of the design procedure used. Signal modulation characteristics of the tube are also discussed in this section.

Design Considerations

While T W T theory served as a general guide in the development of this tube, a number of important tube parameters had to be determined either by experimentation or by judgement based on past experience. The most important of these were:

Saturation power output	12 watts
Mean helix diameter	90 mils
γa	1.6
Magnetic flux density	600 gauss
Cathode current density	200 ma/cm^2

These quantities and the requirement of 30 db gain at five watts output largely determined the T W T design.

The saturation output of 12 watts was found necessary to obtain the desired linearity at five watts output and the γa value of 1.6 to obtain the flattest frequency response over the desired band.

The choice of helix diameter and magnetic flux density represented a compromise. For the highest gain per unit length, best efficiency, and lower operating voltage, a small helix diameter was called for. On the other hand, a large helix diameter was desirable in order to ease the problem of beam focusing and to facilitate the design of a lightweight permanent magnet focusing circuit. In particular, the design of such a circuit can be greatly simplified if the field strength required is less than the coercive force of available magnetic materials. These considerations led to a choice flux density of 600 gauss, thereby permitting use of a magnetic circuit using Alnico bar magnets.

To obtain long tube life, it was desirable to limit the helix interception to about one per cent of the beam current. On the basis of past results it was estimated that

Table 2 — Summary of Design

I	Helix Dimensions			
	Mean Diameter		90 mils	
	Inside Diameter		80 mils	
	Wire Diameter		10 mils	
	Turns per inch		34	
	Pitch		29.4mils	
	Wire Diameter/Pitch		0.34	
	Active Length		5 1/2 inches	
II	Voltages and Currents			
	Electrode	Voltage (volts)	Current (ma)	
	Cathode	0	40	
	Beam Forming Electrode	0	0	
	Accelerator	2600	0.1	
	Helix	2400	0.4	
	Collector	1200	39.5	
	Heater Power	6 watts		
III	T W T Parameters at Midband (6175 mc)			
		1.58		
		0.148		
		0.058		
		0.29		
	N (number of λ's on helix)	30		
	Dielectric Loading factor	0.79		As defined by Tien
	Impedance Reduction factor	0.4		
IV	Electron Gun			
	Gun-type — Converging Pierce Gun			
	Cathode type — Sprayed Oxide			
	Cathode Current Density 213 ma/cm^2		(for I_k = 40 ma)	
	Cathode Diameter — 192 mils			
	Converging half angle 12° 40'			
	Cathode radius of curvature (r_c) 438 mils			
	Anode radius of curvature (r_a) 190 mils			
	r_c / r_a 2.3			
	Perveance 0.3 X 10^{-6} amps / volts $^{3/2}$			
	$(V_A/T_K)^{1/2}$ = 1.61 for T_K = 720°			
	At the beam minimum in absence of magnetic field:			
	r_{min} (from Pierce)		11.5 mils	
			0.220	
	from Danielson, Rosenfeld & Saloom		20.5 mils	
			3.50	
			4.80 mils	

Table 2 (concl.)

	Brillouin flux density for 80 mil helix ID	240 gauss
	Actual focusing flux density required	600 gauss
	Beam transmission from cathode to collector at 5 watts output	99 %
V	R F Performance	
	Frequency range	5925–6425 mc
	Saturation power output	12 watts
	Nominal power output	5 watts
	Gain at 5 watts	31–35 d b
	Noise figure	30 d b
	Input V S W R	1.1 impedance match
	Output V S W R (at 5 watts)	1.4 to WR 159 waveguide

this could be done with a magnetic flux density 2.6 times the Brillouin value for a beam entirely filling the helix. With this restriction, Figure 11 shows how the T W T design is affected by varying the helix diameter. A choice of 600 gauss is seen to result in a mean helix diameter of 90 mils.

In the selection of cathode current density, a compromise between long life and ease of focusing had to be made. To obtain long life, the current density should be minimized. However, this calls for a highly convergent gun which in turn complicates the focusing problem. It was decided to use a sprayed oxide cathode operating at about 200 ma/cm^2. Experience had shown that tube life in excess of 10,000 hours was possible with such a cathode. Moreover, an electron gun of the required convergence (about 13° half angle) could be designed using standard techniques.

The various dimensions, parameters, voltages and currents involved in the design are summarized in Table 11. For the sake of completeness, some r.f. performance data are also included.

Description of the Tube

General Description. This section describes the mechanical structure and presents some performance data closely associated with particular portions of the tube. The overall r.f. performance is reserved for consideration in the next section. It was attempted to achieve a design which could be easily modified for experimental purposes and which could also be adapted to quantity production. To assist in obtaining low gas pressure, a rather "open" structure is used, thereby minimizing the pumping impedance. In addition, all parts are designed to withstand comparatively

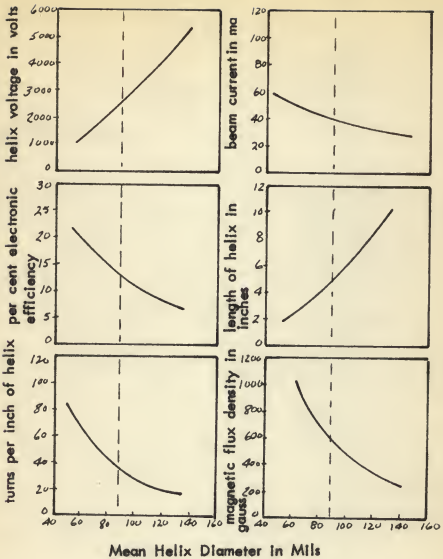

Figure 11 — Alternate designs. These curves are an estimate of how the T W T design would be affected by changing the helix diameter. In all cases the expected maximum power output is 12 watts and the low-level gain is 33 db. The line at 90 mils mean diameter in the curves represents the present design. In these calculations it was assumed that:

a. $r_a = 1.6$
b. power output = $2.1\ C I_0 V_0$ = 12 watts
c. the magnetic flux density is 2.6 times the Brillouin flux density for a beam entirely filling the helix.
d. the ratio of wire diameter to pitch is 0.34
e. the dielectric loading factor is 0.79
f. the ratio of effective beam diameter to mean helix diameter is 0.5

high temperatures during outgassing, both when the tube is pumped and, in the case of the helix and gun assemblies, during a vacuum firing treatment prior to final assembly.

Control of Positive Ions. Experience with previous T W T's has indicated that an improvement in life by as much as a factor of ten is obtained by arranging the d c potential profile so that positive ion bombardment of the cathode is minimized. This improvement has been observed even in tubes in which all reasonable steps have been taken toward minimizing the residual gas pressure. From Table 11 it is seen that the relative values of accelerator, helix, and collector voltage are arranged to drain positive ions formed in the helix region toward the collector. These ions are thereby kept from reaching the cathode. Spurious ion modulation which can result from accumulation of ions in the helix is also minimized.

The effect that ions can have on cathode life was clearly demonstrated in a T W T which was in many aspects a prototype. This tube operated with the accelerator, helix and collector at successively higher voltages, with consequent ion draining toward the cathode. Severe ion bombardment of the cathode brought about failure of most of these tubes in from 500 to 2,000 hours. In contrast to this the average life of this tube was in excess of 10,000 hours in spite of a cathode current density about twice that in the prototype tube. Moreover, failure of the tube comes about from exhaustion of coating material rather than as a result of ion bombardment. During the course of the work of the prototype tube, an experiment was performed to determine how much the ion bombardment would be affected by changing the potential difference between tube electrodes. In this experiment a small hole was

drilled in the center of the cathode and an ion current monitoring electrode placed behind it. The ion monitor current was then investigated as a function of electrode voltages. Figure 12 shows the results. We see that comparatively small potential differences are adequate to control the flow of positive ions.

The Electron Gun and Electron Beam Focusing. The electron gun uses is a converging Pierce gun. The values of the gun parameters are summarized in Table 11. Included are both the original parameters introduced by Pierce as well as those defined in a recent paper by Danielson, Rosenfeld and Saloom in which the effects of thermal velocities are considered. Figure 13 shows a drawing of the electrically significant contours of the gun. The method of constructing the gun is a modification of a procedure used in oscilloscope and television picture tubes. The electrodes are drawn parts made of molybdenum or, in the case of the cathode, of nickel. They are supported by rods which are in turn supported from a ceramic platform to which these rods are glazed. The whole gun structure is supported from the end of the helix by the helix connector detail. Since this part must operate at helix potential, it is insulated from the remainder of the gun by a ceramic cylinder which is glazed both to it and to the accelerator.

To obtain good focusing, the cathode must be accurately aligned with respect to the other electrodes. However, it must be omitted from the gun during the glazing process and during a subsequent vacuum outgassing because the cathode coating can not withstand the temperatures involved.

Initially, it was thought that the cathode should be completely shielded from the magnetic field, and that the field should be introduced in the region between the

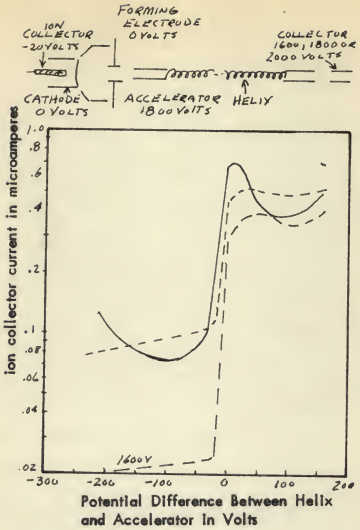

Figure 12 — Effect of electrode voltages on ion bombardment of the cathode. In this experiment the helix voltage was varied while the positive ion current to a monitor electrode behind a hole in the cathode was measured. Curves are shown for the collector voltage greater than, equal to, and less than the accelerator voltage. During this experiment the accelerator voltage was held constant at 1800 volts with a resulting beam current of 40 ma. These curves show that the ion bombardment of the cathode can be reduced by as much as a factor of 20 by properly arranging the voltage profile.

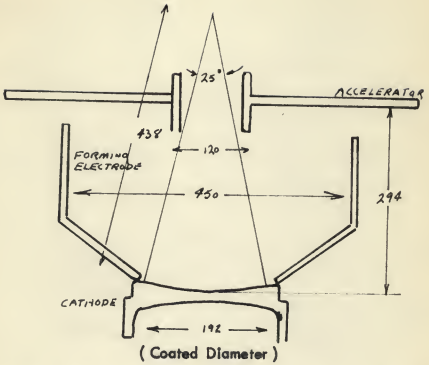

Figure 13 — The electrically significant contours of the gun. All dimensions are in mils. These contours were determined using an electrolytic tank and following the procedure originated by Pierce. The measured potential at the beam boundary in the tank was made to match the calculated value with ± 1/4 per cent of the accelerator voltage to within 10 mils of the anode plane. The aperture in the accelerator was made sufficiently large so that substantially no beam current is intercepted on it. The significant parameters of this gun are:

P = 0.3×10^{-6} amps/volts $^{3/2}$

J = 213 ma/cm^2

accelerator and the point at which the beam would reach its minimum diameter in the absence of magnetic field. This arrangement did result in the best beam transmission to the collector. It was later discovered, however, that the noise on the electron stream became extremely high when there was no magnetic flux at the cathode. This effect will be discussed further in another part. It was found that by having a flux density of about 20 gauss at the cathode, the noise figure could be considerably reduced with the only penalty being a slight increase in interception on the helix. The penalty results from the fact that the flux linking the cathode causes a reduction in the angular velocity of the electrons in the helix region, and this in turn diminished the magnetic focusing force. (Busch's theorem)

Figure 14 shows the distribution of axial magnetic field in the gun region. The curve represents a compromise between that which gives best focusing (zero flux density at the cathode) and that which gives best noise performance (about 25 gauss flux density at the cathode). This flux density variation was derived by empirical methods.

Measurements of beam interception as a function of magnetic flux density are shown for several beam currents in Figure 15. These measurements were obtained without any r.f. input to the T W T.

Applying sufficient r.f. input to drive it into non-linear operation, results in defocusing caused by the high r.f. fields (both from the helix wave and from space charge) near its output end. Figure 16 shows how the beam interception for different magnetic flux densities varies as a function of the power output of the T W T. From these curves one sees that an output level of five watts can be maintained with about one per cent interception with a flux density of 600 gauss.

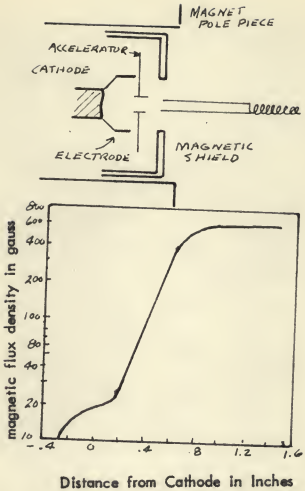

Figure 14 — Variation in magnetic flux density as a function of distance from the cathode. A schematic representation of the gun electrodes and of the magnetic parts which have been used to control the flux is also shown. All the elements inside the tube are non-magnetic so that the flux density variation is determined entirely by magnetic parts external to the tube envelope. The flux density at the cathode is built up (i.e., the step is put into the curve) by having the magnetic shield end near the cathode. The flux which leaves the shield at this point increases the flux density at the cathode over what it would be if the shield extended well behind the cathode.

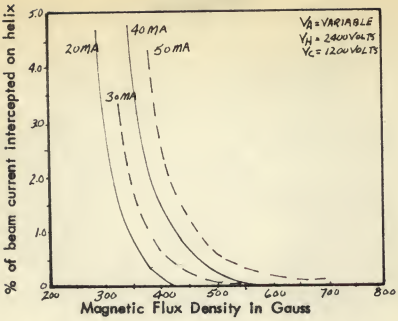

Figure 15 — Per cent interception on the helix as a function of magnetic flux density, These measurements were taken using a precision solenoid to focuss the T W T.

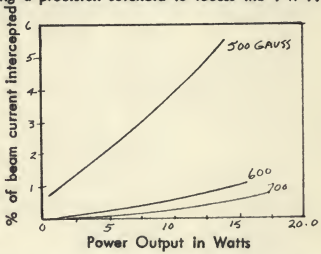

Figure 16 — Per cent interception on the helix as a function of rf power output. These measurements were made using permanent magnet circuits charged to different field strengths.

The Helix. The helix assembly is a rigid self-supporting structure composed of three ceramic support rods bonded with glaze to the helix winding. The support rods are steatite ceramic. This material was chosen because of its low r.f. losses and because these losses do not increase rapidly with temperature. Attenuation is applied over a length of two inches starting 1 1/2 inches from the input and by spraying the helix assembly with aquadag (carbon in water suspension) and then baking it.

Supporting the winding by glazing it to ceramic support rods has the following advantages:

(1) The dielectric loading and intrinsic attenuation of the helix are comparatively low because the amount of supporting structure in the r.f. fields is small.

(2) High loss per unit length in the helix attenuator is made possible. The reason for this will be discussed further below.

(3) The heat dissipation capability of the helix is greatly increased because the glaze provides an intimate thermal contact between winding and support rods.

(4) Mechanical rigidity is realized and therefore the helix can be handled without risk of disturbing the pitch or diameter of the winding.

On the other hand, use of the ceramic rods has a significant disadvantage in that it makes the outside radius of the vacuum envelope large compared to the helix radius, thus making coupled helix matching out of the question. To obtain reproducibility of performance, the helix must be precisely constructed. Together, the pitch of the helix and the amount of dielectric loading determine the synchronous voltage. A pitch variation of ±one per cent results in a voltage variation of about ±50 volts, and a loading variation of ±one per cent results in a variation of about ± 25 volts. It is not difficult to hold the average pitch variations to less

than ± one per cent. The loading, however, is a more difficult problem for not only must the dielectric properties of the support rods and of the glaze material be closely controlled, but attention must also be paid to the size and density of the glaze fillets. The gain of the tube is affected by the amount of loss in the helix attenuator. For the particular loss distribution used a variation of ± 5 db out of a total of 70 db results in a gain variation of about ± 1 db. The helix attenuator depends to a large extent on a conducting "bridge" between helix turns and therefore the amount of attenuation is sensitive to the size and the surface condition of the glass fillets. Thus, the glazing process must be in good control in order to minimize variations in both gain and operating voltage. With present techniques, one is able to hold the voltage for maximum gain to within ± 50 volts of the nominal value. The gain is held to ± 2 db — about half of the spread caused by variations in loss distribution and about half by differences in beam size.

Helix-to-Waveguide Matching. In the helix-to-waveguide transducer the helix passes through the center of the broad face of the waveguide and energy is coupled between helix and waveguide by an antenna and matching taper. A capacitive coupler on the helix and an r.f. choke on the waveguide place an effective ground plane at the waveguide end of the antenna length. The r.f. choke also assists in minimizing leakage of r.f. power.

The dimensions of this transducer were determined empirically. It was found that the antenna length affects mainly the conductive component of the admittance referred to the plane of the helix. The length of the matching taper affects mainly the susceptive component, and the distance from helix to a shorting plunger, which

closes off one end of the waveguide, affects both components. If the position of the waveguide along the axis of the T W T and the position of the shorting plunger are optimized, the V S W R of the transducer will be less than 1.1 over the entire band. With these positions fixed at their best average value, the V S W R will be less than about 1.3.

Internal Reflections. A problem that required considerable effort was that of "internal reflections". By this it is meant reflections of the r.f. signal from various points along the helix as contrasted with reflections from helix-to-waveguide transducers. The principal sources of internal reflections are the edge of the helix attenuator and small variations in pitch along the helix.

The type of performance degradation caused by small internal reflections can be illustrated by the following. Consider a signal incident on the T W T output as a result of a reflection from a radio relay antenna. Except for a small reflection at the transducer, energy incident on the T W T output will be transferred to the helix, propagated back toward the input, and for the most part be absorbed in the helix attenuator. However, if there are reflection points along the helix, reflected signals will be returned to the output having been amplified in the process by the T W T interaction. Because of this amplification, even a small reflection of the backward traveling wave can result in a large reflected signal at the T W T output.

If there is a long length of waveguide between the T W T and the antenna, the echo signal resulting from a reflection at the antenna and a second reflection at the T W T will vary in phase with respect to the primary signal as frequency is changed. This will cause ripples in both the gain and in the phase delay of the

system as function of frequency. Suppose the V S W R of the antenna is 1.2 and that of the T W T is 1.4 and the two are separated by 100 feet of waveguide. The amplitude of the gain fluctuations will be about 0.25 d b, the amplitude of the phase fluctuations will be about 0.9 degree and the periodicity of the fluctuations will be about six mc. This effect may be eliminated by using an isolator between the T W T and the antenna to eliminate the echo signal.

In addition to echo signals that occur between the T W T and the antenna there are echoes which occur wholly within the T W T as a result of a reflection of the signal from the output transducer and a second reflection from some point along the helix. Thus even if a T W T is operating into a matched load it may have ripples in gain of phase characteristics. These ripples may be controlled by minimizing the internal reflections. In this tube they are less than $\pm$ 0.1 d b in gain and one-half degree in phase. Their perodicity is about 100 mc.

In addition to causing transmission distortions, internal reflections can seriously reduce the margin of a T W T against oscillation. Outside of the frequency band of interest, the helix-to-waveguide transducer may be a poor match or the T W T may even be operating into a short circuit in the form of a reflection type bandpass filter. At such frequencies, the internal reflections must not be large enough so that an echo between transducer or filter and an internal reflection point will see any net gain, or else the T W T will oscillate.

With many types of helix winding equipment, variations in helix pitch are periodic in nature. This causes the helix to exhibit a filter-like behavior with respect to internal reflections. At frequencies at which the period of the pitch variations is an integral number of half-wave lengths, the resultant reflections from each indi-

vidual period will add in phase, thereby causing the helix to be strongly reflecting at these frequencies.

In this tube the situation has been considerably improved by increased precision in the helix winding and by insuring that the remaining periodicity does not produce a major reflection peak in the band.

The Collector. It is desirable to operate the collector at the lowest possible voltage in order to minimize the d.c. power input to the T W T. This increases the overall efficiency and simplifies the collector cooling problem. On the other hand, if there are appreciable potential differences between helix and collector, we must insure that few secondary or reflected electrons return from the collector to bombard the helix and accelerator, or else we may overheat these electrodes. Figure 17 shows a drawing of the collector used. It takes the form of a long hollow cylinder shielded from the magnetic field. Inside of the collector the beam is allowed to gradually diverge and the electrons strike the walls at a grazing angle. This design reduces secondary electrons returned from the collector to almost negligible proportions.

Figure 18 shows the total accelerator and helix interception as functions of collector voltage at various output levels. When there is no r.f. drive, the intercepted current remains low to a collector voltage of about 200 volts at which point it suddenly increases to a high value. This appears to be caused by the phenomenon of space charge blocking. As the collector voltage is progressively lowered, the space charge density at the mouth of the collector increases because of the decrease in electron velocity at this point. Increasing the charge density causes the potential depression in the beam to increase until at some collector voltage the potential on

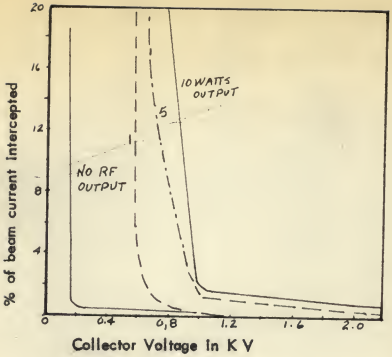

Figure 18 — Intercepted current as a function of collector voltage with helix and accelerator voltages held constant at their nominal values. Below the knee of the curves about three quarters of the total intercepted current goes to the helix and about one quarter is focused all the way back to the accelerator.

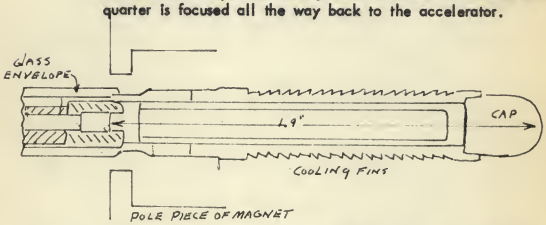

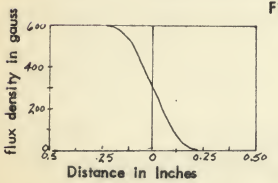

Figure 17 — The collector. The magnetic field variation in the collector region is plotted to the same scale as the collector drawing. The electron beam diverges gradually inside of the collector and the electrons strike the walls at a grazing angle. With this design there are essentially no secondary electrons returned from the collector.

the axis is reduced to cathode potential. At collector voltages lower than this, some of the beam is blocked, i.e., it is turned back by the space charge fields.

When the T W T is operated at appreciable r.f. output levels, the collector voltage must be increased to permit collection of all electrons which have been slowed down by the r.f. interaction. Unfortunately, some electrons are slowed far more than is the average, so that one must apply to the T W T several times more d.c. power than can be taken from it in the form of r.f. power. However, as seen from Figure 18, there is still an appreciable advantage to be gained by operating the collector at lower than helix potential. These curves should not be taken as an accurate measure of the velocity distribution because there are undoubtedly space charge blocking effects which even at higher collector voltages have some influence on the number of electrons returned from the collector. This arises from the fact that the r.f. interaction causes an axial bunching of the electrons, thereby causing the space charge density in an electron bunch to be much higher than it is in an unmodulated beam. Thus, as a bunch enters the collector, the local space charge density may be high enough to return some electrons.

Performance Characteristics

In this section the overall r.f. performance comparisons between theory and observed results will be considered. The following T W T parameters can be varied: input level; helix voltage; beam current; frequency; and magnetic field. The approach here will be to first consider the operation of the tube under what might be called nominal conditions. This will be followed by a discussion of the variations in low-level gain and in maximum output over an extended range of beam current,

frequency, and magnetic field. By this procedure one is able to obtain a description of tube performance without presentation of a formidable number of curves.

Nominal conditions refer to the following:

frequency	6000 mc (band center)
beam current	40 ma
magnetic flux density	600 gauss
collector voltage	1200 volts

Figure 19 shows representative curves of output power as a function of input power for several values of helix voltage. This information is replotted in Figure 19(b) in terms of gain as a function of output power. As may be seen the T W T operates as a linear amplifier for low output levels. As the output level is increased, the tube goes into compression and finally a saturation level is reached. The maximum gain at low input levels is obtained with a helix voltage of 2,400 volts (about 12 per cent higher than the synchronous voltage because of space charge effects).

The maximum output at saturation is obtained at a higher helix voltage as is common in T W T's. The helix voltage also affects the shape of the input-output curves — linear operation being maintained to higher output levels at higher helix voltages.

The efficiency of electronic interaction in a T W T (electric efficiency) is defined as the ratio of the r.f. output power to the beam power (product of helix voltage and beam current). The over-all efficiency is defined as the ratio of the r.f. output power to the total d.c. power (exclusive of heater power) delivered to the tube. With the collector operated at 1,200 volts, it is about twice the electronic efficiency. The electronic and over-all efficiencies there are equal to

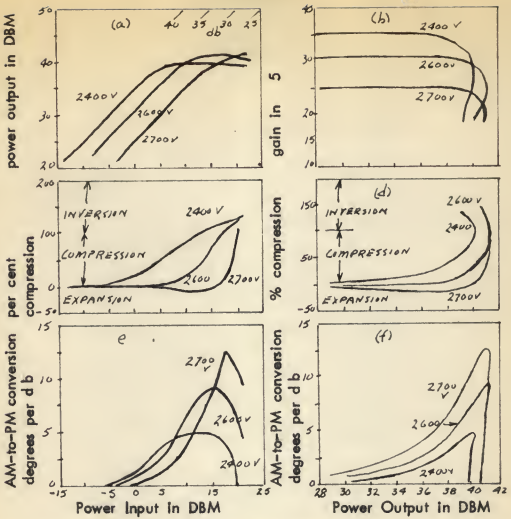

Figure 19 — (a) Output power as a function of input power. Both ordinate and abscissa are in dbm (db with respect to a reference level of one milliwatt). A straight line at 45° represents a constant gain. A gain scale is included along the top of the figure. For this tube a helix voltages of 2,400 volts gives maximum gain at low signal levels and a voltage of about 2,600 gives maximum output at saturation.

(b) Gain as a function of output power. This is an alternate way of presenting the information shown in (a).

(c) Compression as a function of input power. Three regions are shown in the figure. The "compression" region is that in which there is less than one db change in output level for a db change in input level. The "expansion" region is that in which there is more than one db change in output level for a db change in input level. The "inversion" region is that in which the output level decreases when the input level increases (or vice versa). It occurs for input levels greater than that necessary to drive the T W T to saturation.

(d) Compression as a function of output power.

(e) Conversion of AM to PM as a function of input power

(f) Conversion of AM to PM as a function of output power

about 14 per cent and 28 per cent respectively.

The curves of Figures 19 (a) and (b) were taken with sufficient time allowed for the tube to stabilize at each power level. If the T W T is driven to a high output level after having been operated for several minutes with no input signal, the output will be somewhat greater than is shown in the curves. It will gradually decrease until it reaches a stable level in a period of about two minutes. This "fade" is caused by an increase in the intrinsic attenuation of the helix near the output end. The increase is a result of heating from r.f. power dissipation. At maximum output the fade is about 0.6 d b (about 15 per cent decrease in output power).

Distortion of the Modulation Envelope. The curves of Figure 19 (a) and (b) tell what happens when a single frequency carrier signal is passed through the T W T. In addition one would like to know the effect on modulation which may be present on the signal. In particular, it is desirable to know the compression of the envelope of an A M signal and the amount of phase modulation generated in the output signal as a result of amplitude modulation of the input signal, (an effect commonly known as A M-toP M conversion). As a measure of compression of an A M signal the quantity per cent compression will be used. This is defined as

$$\% \text{ Compression} = \left[1 - \frac{\Delta V_o/V_o}{\Delta V_i/V_i}\right]100$$

where V_o is the voltage of the output wave, V_i is the voltage of the input wave, and V_o is the change in output voltage for a small change in V_i in the input voltage. When $\Delta V_i/V_o$ is small it can be expressed in d b as $8.68\ \Delta V_i/V_o = \Delta V_i/V_o$ in d b. From this it follows that

$$\% \text{ Compression} = \left[1 - \frac{\Delta P_o}{\Delta P_i}\Big\}\text{ in db}\right]100$$

where P_o is the change in output power for a change P_i in input power, and the two powers are measured on a d b scale. When the per cent compression is zero the T W T is operating as a linear amplifier; when it is 100 per cent the T W T is operating as a limiter.

From the above expression it may appear that the per cent compression could be determined directly from the slope of the input-output curves. This would be the case were it not for fading effects. Since there is fading, however, the slope for rapid input level changes is different at high levels from the slope of the static curves. This is necessary to determine compression from the resulting effect on an A M signal.

The electric length of a T W T operated in the non-linear region is to some extent dependent on the input level. Therefore, an A M signal applied to the input of the T W T will produce phase modulation (P M) of the output signal. This effect may be of particular concern when a T W T operating at high output levels is used to amplify a low-index F M signal. If such a signal contains residual amplitude modulation, the T W T generates phase modulation with phase deviation proportional to the input amplitude variation. Under certain circumstances this can cause severe interference with the signal being transmitted. A particular example of this will be discussed after consideration of the compression and A M-to-P M conversion characteristics of this tube.

As in the case of compression, one must measure A M-to-P M conversion dynamically. This is necessary because point-by-point measurements of the shift in output phase as input level is changed include a component of phase shift caused by change in temperature of the ceramic support rods and a consequent change in

their dielectric constant. However, this thermal effect does not follow A M rates of interest and therefore does not produce A M-to-P M conversion.

Compression is given as a function of power input in Figure 19 (c) and as a function of power output in Figure 19 (d). It is seen that compression sets in more suddenly at higher helix voltages. Above about 2,500 volts there is expansion for some values of power input. Figures 19 (e) and (f) give the A M-to-P M conversion as function of input and output power respectively. These data indicate that the conversion is very much less if the tube is operated at lower helix voltages. For example, the conversion at the saturation level of the 2,700 volt curve is about 2 1/2 times that for the 2,400 volt curve.

A final method of plotting gain, compression and A M-to-P M conversion data is shown in Figure 20. The abscissa here is the helix voltage. For these measurements power output was held constant by adjusting input level at each voltage. The figure shows that as helix voltage is increased, the compression decreases but the A M-to-P M conversion increases. The choice of a helix voltage at which to operate the tube must therefore represent a compromise between these quantities.

Significance of A M-to-P M Conversion. In this section we shall consider some of the consequences of A M-toP M conversion. As an example, we will consider the case of a low-index F M signal. Assume the frequency deviation is ±5 mc peak to peak. This gives a phase deviation of ±0.5 radian for a 10 mc modulating signal. These values are typical of what might be found in a radio relay system. Also there is a residual amplitude modulation of one d b (about 13 per cent) in the signal and suppose further that the signal is amplified by a T W T having a value

of A M-to-P M conversion of 10 degrees per d b. Thus, phase modulation thus created in the T W T can either add to or subtract from that of the original F M signal, thus changing its modulation index. At low modulation signal frequencies the phase deviation of the F M signal will be large compared to that of the P M interference and the interference will be of little consequence. At high modulation signal frequencies the phase deviation of the original F M and of the interfering P M signals will be compared and the interference can considerably change the net phase deviation of the overall signal. For the example we are considering the frequency response in Figure 20, which shows what could be seen at the output F M terminal. Curves are given both for the P M interference adding to and subtracting from the original F M signal. It can be seen that a gain-frequency slope of about 4 d b over 10 mc is introduced by A M-to-P M conversion. To prevent such an effect a limiter should be used prior to the T W T in application of this nature so as to remove the offending A M from the input signal.

The fact that compression and amplitude-to-phase conversion vary with input level means that in addition to the first order distortion just described, higher order distortions of the modulation envelope will occur. If, for example, the input signal is amplitude modulated at frequency f_1, the output modulation envelope will contain amplitude and phase modulation both at f_1 and at harmonics of f_1. The amount of higher order distortion can be estimated by expanding the compression and amplitude-to-phase conversion curves as a function of power input in a Taylor series about the operating point. Such an expansion shows that the greater the slope of these curves the greater will be the higher order distortion.

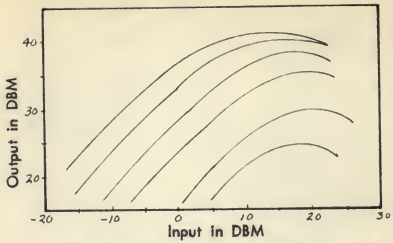

Figure 21 — Output power as a function of input power at various beam currents.

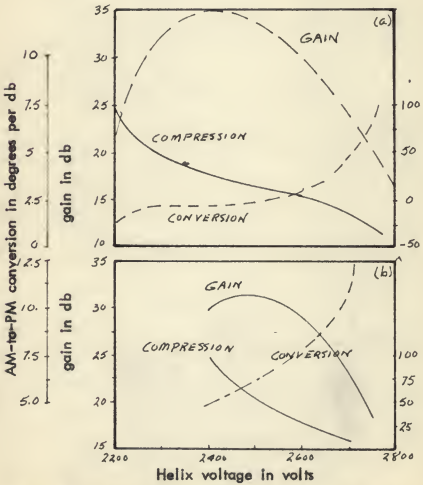

Figure 20 — Gain, compression and amplitude to phase conversion as a function of helix voltage with the output power maintained constant at a level of five watts (a) and ten watts (b).

Extended Range Operation. One can now turn to a consideration of the characteristics over an extended range of beam current, frequency, and magnetic field. Attention will be concentrated on two items, the low-level gain and the maximum power output. From variations in these quantities the complete compression curves can be roughly deduced. This situation is illustrated in Figure 21 which shows output as a function of input at different beam currents. While the shapes of these curves are slightly different for the most part they can be derived from the 40 ma curve by shifting it along the abscissa by the amount the low-level gain changes, and along the ordinate by the amount the maximum output changes as beam current is varied. A similar procedure can be followed for variations with frequency and magnetic field. In all figures in this section, parameters not being purposely varied were held at the nominal values.

Low-Level Gain. Figure 22 shows the variation in low-level gain with beam current and Figure 23 shows its variation with helix voltage for several different beam currents. Figure 24 shows the variation with frequency and Figure 25 the variation with magnetic field.

The observed gain compares well with that calculated from low-level T W T theory provided that we properly consider the effect of the helix attenuator and provided that we assume a b/a of one-half. Figure 26 compares the measured and calculated gain as a function of beam current and Figure 27 compares them as a function of frequency. Figure 28 shows measured and calculated ratios of voltage for maximum gain to synchronous voltage as a function of beam current. In all these figures calculations are shown for several values of the ratio of effective

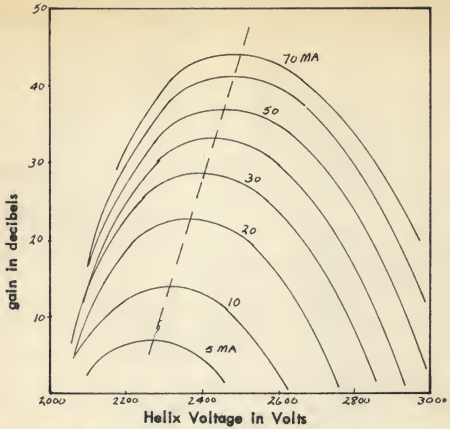

Figure 23 — Low-level gain as a function of helix voltage for various beam currents.

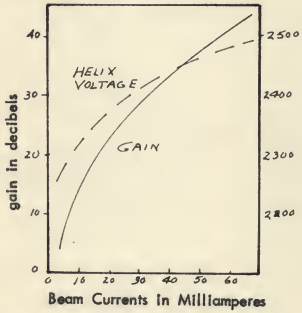

Figure 22 — Low-level gain as a function of beam current

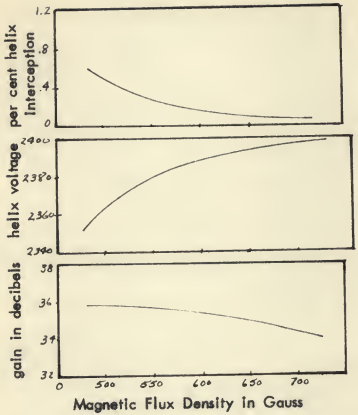

Figure 25 — Low-level gain, helix voltage for maximum gain and helix interception at low signal level as functions of magnetic flux density. The gain varies with magnetic flux density mainly as a result of its effect on beam size and therefore on the degree of coupling between electron stream and helix. The helix voltage varies because of the effect of beam size on QC and therefore on the ratio of the optimum gain voltage to the helix synchronous voltage.

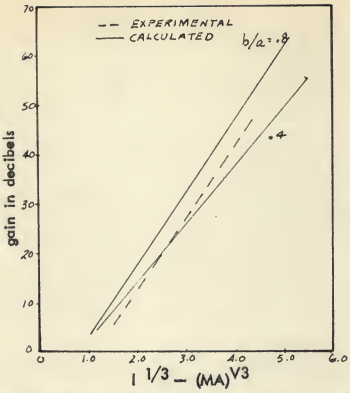

Figure 26 — Measured and calculated low-level gain as a function of the one-third power of beam current.

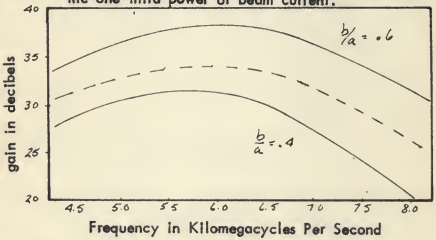

Figure 27 — Measured and calculated frequency response for a current of 40 ma. The parameter b/a is the ratio of effective beam diameter to mean helix diameter.

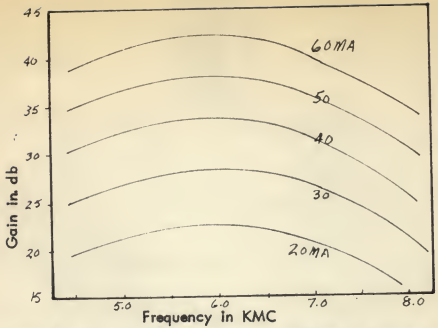

Figure 24 — Low-level gain and helix voltage for maximum gain as functions of frequency for several beam currents.

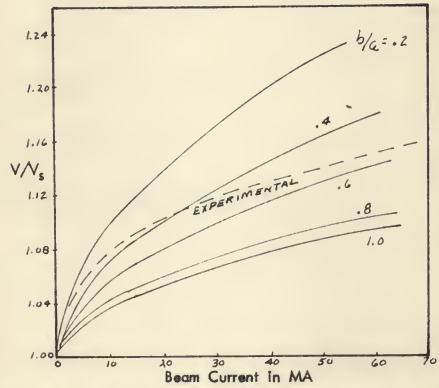

Figure 28 — Measured and calculated ratio of voltage for maximum gain to synchronous voltage as a function of beam current. The calculated curves are shown for several values of the ratio of effective beam radius to mean helix radius (b/a). The location of the measured curve among the calculated ones is taken as an indication of the effective value of b/a. At 40 ma it is about 0.5.

beam diameter to mean helix diameter (b/a). We see that the effective value of b/a appears to be about one-half. On the basis of measurements made by probing the beam of a scaled up version of a focusing system similar to that employed in the tube, the actual beam diameter (for 99 per cent of the current) was found to be about 65 mils (b/a = 0.7). However, the current density distribution is peaked at the center of the beam because of the effect of thermal velocities of the electrons. Thus an effective b/a of 0.5 is not unreasonable.

Maximum Power Output. Figure 29 shows the maximum power output as a function of beam current both immediately after r.f drive is applied and after the tube has had time to stabilize. We see that at high r.f power output the fading becomes very serious and eventually limits the T W T output to about 30 watts. The maximum power output after fading is shown as a function of frequency for several beam currents in Figure 30 and as a function of magnetic flux density in Figure 31.

The theory of the high level behavior of a T W T predicts that the ratio of electronic efficiency (i.e., E= power output/beam power) to the gain parameter C should be a function of C, Q C and b (where b is the beam diameter). However, with the range of parameters encountered in this tube, the variation in E/C should be small. Figure 32 (a) shows E/C as a function of frequency when the T W T is operating at the voltage for maximum gain at low signal levels. Figure 32 (b) shows the maximum value of E/C obtainable at elevated helix voltage. In both figures we show the efficiency as estimated using the results of Tien corrected for the effect of intrinsic loss following the procedure of Culter and Brangaccio.

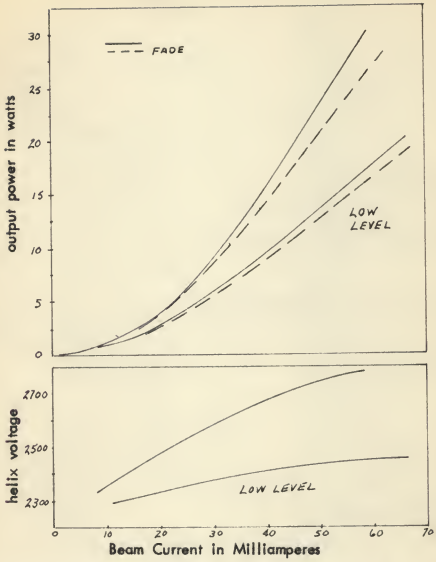

Figure 29 — Maximum power output and helix voltage as functions of beam current. Curves are shown for before and after fading, and for the helix voltage adjusted for the maximum gain at low-level and for maximum output.

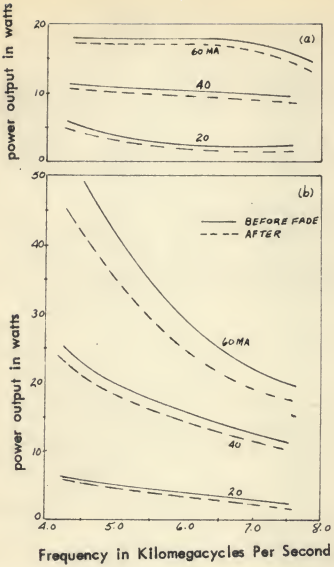

Figure 30 — Maximum power output after fading as a function of frequency for several beam currents; in (a) with the helix voltage adjusted for maximum gain at low-level and in (b) with the helix voltage adjusted for maximum power output.

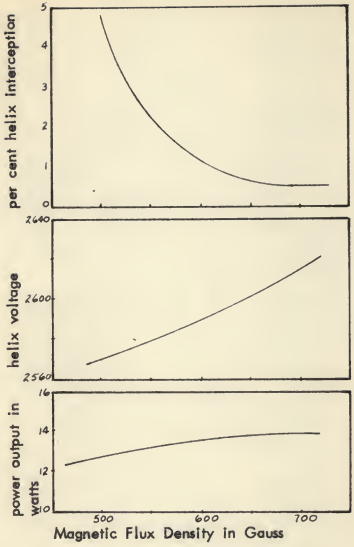

Figure 31 — Maximum power output after fading, voltage for maximum output, and helix interception at maximum output as functions of magnetic flux density.

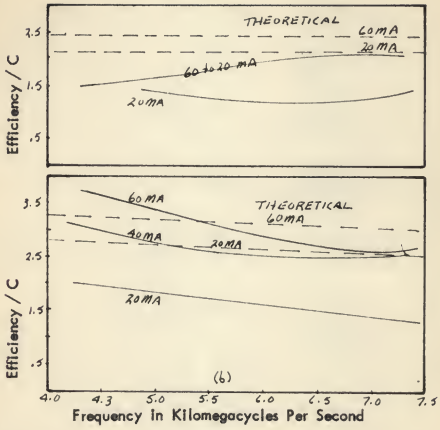

Figure 32 — Ratio of electronic efficiency to gain parameter C as a function of frequency. The efficiencies used for this comparison are all before fading. The dotted lines are estimated from the Tien theory corrected for the intrinsic loss of the helix. The curves in (a) are for the case of the helix voltage adjusted for the maximum low-level gain and those in (b) for the case of the helix voltage adjusted for maximum power output.

All efficiencies in these two figures are the electronic efficiencies before fading. It would be quite difficult to compare the efficiency after fading with theory because the intrinsic attenuation in this case varies along the helix in an unknown manner so that we cannot properly take it into account. From the figures we see that the calculated value of E/C at 6,000 mc and 40 ma is not far from the experimental value but the experimental points show more variation with frequency than is predicted by theory. The low efficiency at 20 ma results from the fact that there is insufficient gain between the helix attenuator and the output. As a result, the T W T "overloads in the attenuation".

ACKNOWLEDGMENT

The author would like to thank Professor Ugo Gagliardi, of the Electrical Engineering department, for his help and guidance in writing this paper and to acknowledge the aid given by Sylvania Electric Products in presenting experimental work accomplished in their laboratories.

REFERENCES

Birdsall, C. K. & Whinnery, J.R., J. Appl. Phys., 314, (1953)

Brangaccio, D. J., & Culter C.C., Factors Affecting T W T Power Capacity, I.R.E. Trans. PGED - 3, June, (1953)

Chu, L. J., and Jackson, J.D., Proc. I.R.E., 853, (1952)

Pierce, J.R., T.W.T.'s, D. Van Nostrand Inc., (1950)

Ramo, S., Phys. Rev., 276, (1939)

Sensiper, S., Electromagnetic Wave Propagation, Sc.D., Thesis, M.I.T., (1951)

Tien, P.K., T W T, Proc. I.R.E. January 1956

Tien, P.K., Large Signal Theory of T W T Amplifiers, B.S.T.J., March 1957

Watkins, D.A., & Siegman, A.E., J. Applied Phys. (1958)

THE DESIGN OF A TRAVELING-WAVE TUBE

by

LARRY LEX MOORE

B.S., Kansas State University, 1959

THE ABSTRACT OF
A THESIS

submitted in partial fulfillment of the

requirements for the degree

MASTER OF SCIENCE

Department of Electrical Engineering

KANSAS STATE UNIVERSITY OF
AGRICULTURE AND APPLIED SCIENCE

1960

This thesis on "The Design of a Traveling-Wave Tube" was written as an introduction to high frequency amplification devices which employ the interaction gain principle. The paper starts with some general comments on traveling-wave tubes and introduces the reader to the components used in their construction. From here the writer has attempted to provide a logical sequence of steps through the theory, theoretical design and the actual fabrication of a traveling-wave tube amplifier.

In the introduction section, information which is helpful to the understanding of traveling-wave tube parameters and experimental material used in their design is presented. It was hoped that this information would help the unfamiliar reader with the understanding of similar material used later in the paper.

Following the introduction the paper deals with traveling-wave tube theory and design. The theory of interaction is derived in a straight-forward way so that the engineer with only a basic knowledge of electromagnetic waves can follow the reasoning. The proof is accomplished by deriving a circuit equation for the effect of the beam on the circuit and an electronic equation for describing the effect of the circuit on the beam. These two equations are then solved for the existing modes produced from this interaction. A generalized design procedure is then outlined.

Finally the actual design of a low power traveling-wave tube amplifier is followed through from elementary design to the experimental results of the constructed tube. In this section comparison is made between theoretical and observed results and the resulting conclusions are discussed.